

# Scaling laws for the bifurcation-escape rate in a nanomechanical resonator

M. Defoort,<sup>1</sup> V. Puller,<sup>2</sup> O. Bourgeois,<sup>1</sup> F. Pistolesi,<sup>2</sup> and E. Collin<sup>1</sup>

<sup>1</sup> *Université Grenoble Alpes, CNRS Institut NÉEL,  
BP 166, 38042 Grenoble Cedex 9, France*

<sup>2</sup> *Univ. Bordeaux, LOMA, UMR 5798, F-33400 Talence, France  
CNRS, LOMA, UMR 5798, F-33400 Talence, France*

We report on experimental and theoretical studies of the fluctuation-induced escape time from a metastable state of a nanomechanical Duffing resonator in cryogenic environment. By tuning in situ the non-linear coefficient  $\gamma$  we could explore a wide range of the parameter space around the bifurcation point, where the metastable state becomes unstable. We measured in a relaxation process the distribution of the escape times. We have been able to verify its exponential distribution and extract the escape rate  $\Gamma$ . We investigated the scaling of  $\Gamma$  with respect to the distance to the bifurcation point and  $\gamma$ , finding an unprecedented quantitative agreement with the theoretical description of the stochastic problem. Simple power scaling laws turn out to hold in a large region of the parameter's space, as anticipated by recent theoretical predictions. These unique findings, implemented in a model dynamical system, are relevant to all systems experiencing under-damped saddle-node bifurcation.

PACS numbers: 85.85.+j, 05.40.-a, 05.10.Gg, 05.70.Ln

Transition from a metastable to a stable state is a phenomenon of ubiquitous interest in science: in thermal equilibrium it is the essence of the activation law in chemistry [1, 2], it underlies nucleation in phase transitions, magnetization reversal in molecular magnets [3], biological switches in cells behavior [4] or RNA dynamics [5], transitions of Josephson junctions [6] or fluctuations in SQUIDS [7], the list being obviously non-exhaustive. More recently the study of escape statistics has been possible also for out-of-equilibrium *dynamical* systems like Penning traps [8], Josephson junctions [9], and nano-electromechanical systems [10–14]: the state-switching effect is extensively used in bifurcation amplifiers, with for instance state-of-the-art quantum bit read-out schemes [15]. In most of these cases the escape time distribution is exponential and the rate  $\Gamma$  characterizes completely the phenomenon. Analytical solutions [16] of the dynamical equations show that its value depends exponentially on a parameter  $D^{-1}$ , that coincides with the (inverse of the) temperature for equilibrium systems and more generally is related to the power spectrum of the relevant fluctuations. One can then write:

$$\Gamma = \Gamma_0 \exp(-E_a/D), \quad (1)$$

where the prefactor  $\Gamma_0$  is assumed to depend very weakly on  $D$ , and  $E_a$  in analogy with a potential system can be called activation energy: it parametrizes the distance to the unstable point. For out-of-equilibrium systems a central theoretical result is the paper by Dykman and Krivoglaz [17], that found an explicit expression for  $E_a$  and  $\Gamma_0$  for a generic dynamical system close to the bifurcation point, where the line of metastable states joins the line of unstable ones. It predicts universal power laws dependence of  $E_a$  and  $\Gamma_0$  on the distance from the bifurcation point in terms of  $|\omega - \omega_b|$ , where  $\omega$  is the driving frequency of the dynamical system and  $\omega_b$  is its bifurcation value.

Direct experimental measurement of the escape time and study of the dependence of  $E_a$  and  $\Gamma_0$  over a wide range of a system's parameters is not a trivial task, since the exponential dependence of the escape time makes it either too long or too short for a reasonable observation protocol. For dynamical systems the resonating period fixes a lower bound on the time. Nano-mechanical resonators with resonance frequency in the MHz range are thus a prominent choice to investigate the bifurcation instability of Duffing oscillators: they are high frequency dynamical systems with a high quality factor for which the distance to the bifurcation point can be directly controlled.

In the analysis of switching and reaction rates, three problems can thus be distinguished: obtaining the exponent  $E_a$ , the prefactor  $\Gamma_0$ , and their respective scalings for systems away from thermal equilibrium. The exponent has been the first subject of interest, with the early work of Arrhenius [1]. The prefactor has then been addressed by Kramers later on [2], while finally the scaling of both for dynamical systems has been derived by Dykman [17]. It is actually in micro and nano-mechanical systems that a measurement of the power law dependence of  $E_a$  with respect to the distance from the bifurcation point has been performed, giving the predicted value within experimental error [10, 11]. Nevertheless, the activation energy has been claimed to match theory at best within a factor of 2 due to injected noise calibration [10]. To our knowledge no attempts have been done to obtain a more quantitative verification of the predictions of Dykman and Krivoglaz [17], in particular for the scaling law of the prefactor  $\Gamma_0$  and the dependence to the Duffing non-linear coefficient  $\gamma$  of both  $\Gamma_0$  and  $E_a$ . Answering the three above mentioned problems *together* is thus the aim of our work, using a unique nano-mechanical implementation of the bifurcation phenomenon.

In this Letter we report on experimental and theoretic-

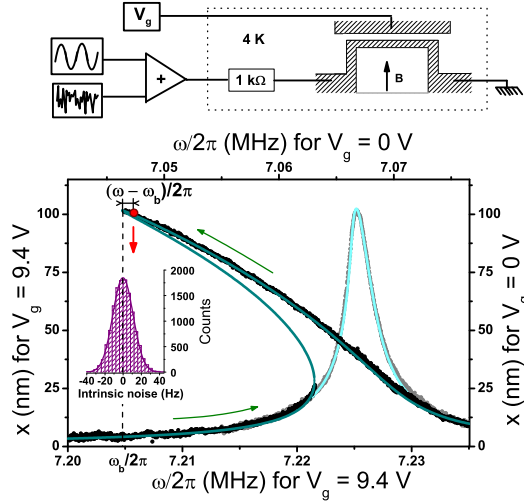


FIG. 1: (Color online) Top panel: Schematic of the experimental setup with the nano-resonator structure. Bottom panel: Linear and Duffing resonances (respectively grey and black points, with top-right and bottom-left axes). The lines show the fit. The nonlinear resonance is for  $V_g = 9.4$  V, which shifts the resonance frequency and opens an hysteresis (thin green arrows highlight upward and downward sweeps). The relaxations occur at a detuning  $\omega - \omega_b$  from the bifurcation frequency (red point and vertical arrow). Inset: Gaussian distribution histogram of the measured intrinsic frequency fluctuations.

cal investigations of the dependence of  $E_a$  and  $\Gamma_0$  on the system parameters for a driven nano-mechanical oscillator in the non-linear regime in presence of a controlled noise force. It is well known that for a sufficiently strong non-linear term the system admits for some values of the driving frequency a metastable solution. By measuring the escape rate for a wide range of parameters we could verify the validity of the power scaling laws predicted by Dykman and Krivoglaz for both  $E_a$  and  $\Gamma_0$ . Remarkably, we found that the scaling holds experimentally in a much larger region of the parameter space than the one for which the theory of Ref. [17] has been derived. Concerning the  $E_a$  dependence on detuning, the possibility of an extended region of scaling was discussed in Refs. [18, 19]. Performing the full numerical simulation of the stochastic problem adapted to our device parameters we found that experiment and theory are in excellent quantitative agreement.

The experiment is performed on a unique goalpost (depicted in top graph of Fig. 1) aluminum-coated silicon nano-electro-mechanical resonator. It consists in two cantilever feet of length  $3 \mu\text{m}$  linked by a paddle of length  $7 \mu\text{m}$ , all about  $250 \text{ nm}$  wide and  $150 \text{ nm}$  thick for a total mass  $m = 1.25 \cdot 10^{-15} \text{ kg}$  [20]. The experiment is performed at  $4.2 \text{ K}$  in cryogenic vacuum (pressure  $< 10^{-6} \text{ mbar}$ ). The motion is actuated and detected by means of the magnetomotive scheme [21], with a magnetic field

$B < 1 \text{ T}$  and a gate electrode is also capacitively coupled to the nanomechanical device (gap about  $100 \text{ nm}$ ) [20]. The resonator admits large distortions (in the hundred nm range) to be attained while remaining intrinsically extremely linear [22], while a well-controlled non-linearity can be generated by means of a DC gate voltage bias  $V_g$  [23]. This distinctive feature enables to tune the global non-linearity of our device without changing the displacement amplitude. Using an adder we apply both a sinusoidal drive and a noise voltage from a voltage source generator. The resulting electric signal together with a  $1 \text{ k}\Omega$  bias resistor is used to inject an AC current through the goalpost and generates both driving and controllable (zero average) noise forces on the resonator. More information on the calibration and experimental details can be found in Refs. [20, 22]. The resulting equation of motion for the resonator displacement  $x$  reads:

$$\ddot{x} + \Delta\omega\dot{x} + \omega_0^2x + \gamma x^3 = f_d \cos(\omega t) + f_n(t) \quad (2)$$

with  $\omega_0/2\pi = 7.07 \text{ MHz}$  the resonance frequency,  $\Delta\omega/2\pi = 1.84 \text{ kHz}$  the linewidth, and  $f_d$  and  $f_n$  the drive and noise forces divided by the mass of the resonator. We fix the drive force so that  $mf_d = 65 \text{ pN}$ , leading to a constant maximal displacement amplitude of  $100 \text{ nm}$ . As can be deduced from our characterizations [20], this amplitude is small enough to guarantee that nonlinear damping mechanisms such as discussed in Refs. [24, 25] are small (see comment in the discussion section). The noise force signal is filtered so that the force spectrum  $\int dt e^{i\omega t} \langle f_n(t) f_n(0) \rangle_\omega = 2D$  is constant over a bandwidth of  $1 \text{ MHz}$  around  $7 \text{ MHz}$ . The Duffing coefficient  $\gamma$  scales as  $V_g^2$  and is for us negative [22]. At fixed driving force, the system admits two amplitudes of oscillation for sufficiently large  $|\gamma|$  as shown in Fig. 1 (bistability). By fitting with the standard Duffing expressions [26] the parameters  $\Delta\omega$ ,  $\omega_0$  and  $\gamma$  together with the bifurcation frequency  $\omega_b$  can be obtained with a good accuracy. The experiment is then performed by sweeping  $\omega$  from the stable regime ( $\omega > \omega_0$ ) down to the edge of the hysteresis at a given value of  $\omega - \omega_b$  in the high amplitude state (see Fig. 1). The sweeping rate (a few Hz/s) is an important parameter which should both guarantee adiabaticity of the sweep and high accuracy in the measurement [33]. Finally, the escape time from the metastable state is detected when the measured displacement amplitude falls below an appropriate threshold value. Typically  $10^3$  escape events are recorded for each set of parameters. The experiment has been repeated for three different values of the noise forces  $f_n$ , three different detunings  $\omega - \omega_b$  (up to 5% of the hysteresis), and five different values of  $V_g$  (and thus of  $\gamma$ ), for a total of 45 escape histograms. The resulting settings are summarized in Fig. 2.

For each data measurement, the experimental value of  $\omega_b$  might slightly differ from the one obtained by the initial fit. This problem is detected by sweeping relatively rapidly  $\omega$  (tens of Hz/sec) through the bifurcation point and measuring the escape value  $\omega_b$  prior to

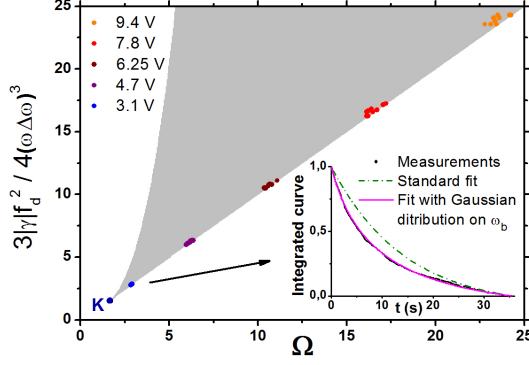


FIG. 2: (Color online) Bifurcation parameter space (normalized driving force versus  $\Omega = 2|\omega - \omega_0|/\Delta\omega$ ). The grey area is the NEMS bistability regime where the right edge is the transition from a high amplitude oscillation to a low one (the left edge is the opposite) and K is the spinode point where hysteresis starts to open. We show within the bistability the data points at different voltages  $V_g$ . Inset: typical low  $V_g$  relaxation curve obtained with about 1000 relaxations, and fit with and without fluctuations on  $\omega_b$ .

each relaxation-time acquisition. A typical histogram of the distribution of  $\omega_b$  is shown in the inset of Fig. 1 for  $V_g = 9.4$  V. It has Gaussian form with a half-width  $\sigma$  in the range of tens of Hz. This tiny spread ( $10^{-6}$  to  $10^{-5}$  of  $\omega_b$ ) is due to low-frequency intrinsic fluctuations of the resonating frequency, which actual origin is still under debate [27–29]. Even if extremely small, due to the high sensitivity of the bifurcation phenomenon the fluctuations of  $\omega_b$  modify slightly the value of  $\Gamma$  at each measurement, and we have to take this effect into account. The escape exponential distribution has thus to be averaged over these fluctuations. For  $|\omega - \omega_b| \gg \sigma$  one can expand this dependence:  $\Gamma(\omega - \omega_b - \epsilon) = \Gamma + \Gamma'\epsilon + \dots$ , where  $\epsilon$  is the Gaussian-distributed shift of  $\omega_b$ . This gives the following distribution for the escape times:

$$P(t) = \Gamma e^{-\Gamma t} \int \frac{d\epsilon}{\sigma\sqrt{2\pi}} e^{-\epsilon^2/(2\sigma^2) - \Gamma'\epsilon t}. \quad (3)$$

Fitting it to the data with the method of Kolmogorov-Smirnov [30], to avoid losses of information due to histogram binning, the two independent parameters of the distribution,  $\Gamma$  and the product  $\Gamma'\sigma$ , can be obtained. A typical curve is shown in the inset of Fig. 2. Note that this procedure does not need any hypothesis on the explicit functional dependence of  $\Gamma$  on  $\omega_b$ . On the other hand the procedure breaks down for too small detunings, and we thus need to drop the data for four values of the detuning. We can then verify the validity of Eq. (1) for the system at hand by plotting  $\log \Gamma$  as a function of  $1/D$  (see Fig. 3). The linear fit gives  $E_a$  and  $\Gamma_0$ . The absolute experimental definition of the noise level is difficult, and we introduce a calibration factor  $C$  (close to 1) between  $D$  and the nominal injected noise power. Note that it simply amounts to multiply  $E_a$  by  $C$ , thus leaving the

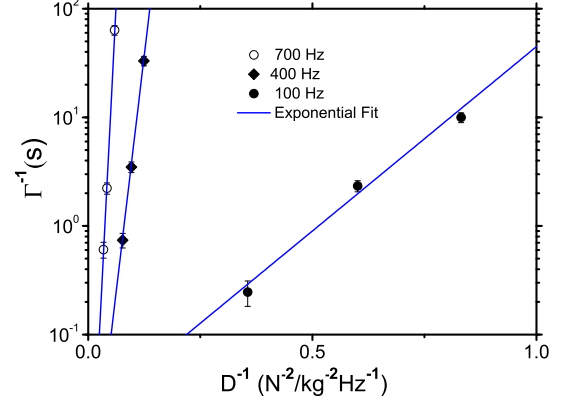


FIG. 3: (Color online) Escape time as a function of  $D^{-1}$  for  $V_g = 9.4$  V at different detunings  $\omega - \omega_b$  from the bifurcation point.

scaling dependence unmodified. The value of  $\Gamma_0$  is not affected by this calibration either. More experimental details can be found in Ref. [31].

In order to extract the scaling dependence of  $E_a$  and  $\Gamma_0$  on the detuning and the non-linear parameter  $\gamma$  it is convenient to recall the predictions that can be obtained following Ref. [17]. Let us rescale the detuning by defining  $\Omega = 2|\omega - \omega_0|/\Delta\omega$  with  $\Omega_b = 2|\omega_b - \omega_0|/\Delta\omega$ . For  $\Omega_b \gg \sqrt{3}$  (that holds for all the data of our experiment) one obtains that  $\Omega_b \approx 3|\gamma|f_d^2/(4\omega^2\Delta\omega^2)$  with the parameters in Eq. (1) reading [34]:

$$E_a = \frac{2f_d^2}{3\Delta\omega} \frac{|\Omega - \Omega_b|^{3/2}}{\Omega_b^{5/2}}, \quad \Gamma_0 = \frac{\Delta\omega}{2} \frac{|\Omega - \Omega_b|^{1/2}\Omega_b^{1/2}}{2\pi}. \quad (4)$$

The basic assumptions to obtain these expressions are that  $E_a/D \gg 1$  in order to keep the escape a rare event, and to be able to reduce this two-dimensional problem (amplitude and phase) into a one-dimensional one. This second condition (much less appreciated in the literature) is only verified when the driving frequency  $\omega$  is in a tiny region close to the bifurcation point  $\omega_b$  and far from the frequency for which the amplitude is maximum. In this region, one of the eigenvalues of the linearized dynamical equations of motion vanishes, which induces a slow motion in the direction of the relative eigenvector. On the other hand when  $\omega$  is such that the amplitude is maximal, the two eigenvalues coincide, inducing fully two-dimensional fluctuations. Thus beyond this point the approximation used to obtain Eq. (4) breaks down. This condition reads  $4\Omega_b|\Omega - \Omega_b| \ll 1$ .

In the experiment we performed this quantity ranged uniformly between 0.13 to 71, thus a part of the data where well outside the range of the expected validity of Eq. (4), enabling to investigate the behavior of  $\Gamma$  in a region where no present analytical prediction exists. As explained, the expressions for  $E_a$  and  $\Gamma_0$  in Eq. (4) de-

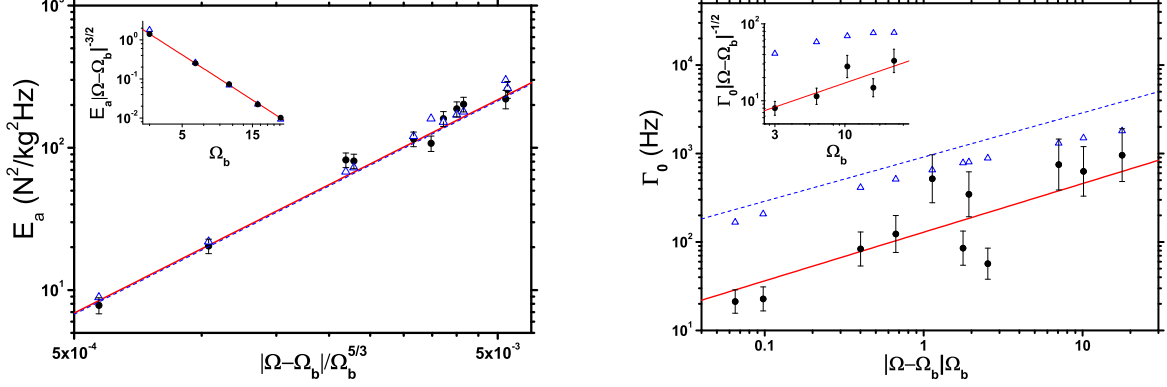


FIG. 4: (Color online) Scaling plots for  $E_a$  (left) and  $\Gamma_0$  (right) with respect to detuning. The full circles indicate the experimental points, the open (blue) triangles the prediction of the full numerical simulation, the (red) full lines the linear fit to the data, and the dashed (blue) lines the prediction of Eq. (4). Insets: scaling with the non-linear parameter  $\Omega_b$ .

pend only on the detuning and the non linear coefficient (through  $\Omega_b$ ), the other parameters being the same for all data points. To test the validity of Dykman-Krivoglaz expressions, we produce a scaling plot, where the logarithm of  $E_a$  and  $\Gamma_0$  are plotted as a function of  $|\Omega - \Omega_b|/\Omega_b^{5/3}$  and  $|\Omega - \Omega_b|\Omega_b$  (see Fig. 4). A remarkable scaling is then observed in all the experimental range, with a fitted slope as a function of the detuning of  $1.53 \pm 0.04$  and  $0.55 \pm 0.2$ , for  $E_a$  and  $\Gamma_0$  respectively. This matches the analytic predictions by Dykman and Krivoglaz, and we use this good agreement to define the noise source calibration factor  $C$ : scaling  $D$  by  $C$  the prediction of Eq. (4) coincides with the fitted value for  $E_a$  (dashed line in Fig. 4 left panel). The dependence on the non-linear parameter  $\Omega_b$  could also be tested for both quantities. It is shown in the insets of Fig. 4 and gives fitted slopes of  $-2.43 \pm 0.05$  and  $0.6 \pm 0.1$ , again in excellent agreement with Eq. (4).

To better understand this remarkable scaling in such a large parameter region we solved numerically the stochastic problem. This can be done by introducing the complex slow amplitude  $z(t)$  defined as  $x(t) = z(t)e^{i\omega t} + z(t)^*e^{-i\omega t}$  and then convert the Langevin Eq. (2) to a Fokker-Planck equation  $\partial_\tau P = \mathcal{L}P$  for the probability density  $P(u, v, \tau)$  of the real and imaginary part of  $z = (3|\gamma|/\Delta\omega)^{1/2}(u + iv)$  as a function of the dimensionless time  $\tau = t\Delta\omega$ . The escape rate from a given domain can be calculated by solving the equation  $\mathcal{L}^\dagger \tau(u, v) = -1$  with zero boundary condition at the border of the domain [16]. This gives the average time needed to reach the border starting at  $(u, v)$ . The equation reads explicitly:

$$[\mathcal{D}(\partial_u^2 + \partial_v^2) - f_u \partial_u - f_v \partial_v] \tau = -1, \quad (5)$$

with  $\mathcal{D} = 3|\gamma|D/(8\omega^3\Delta\omega)$ ,  $f_u = u + v(u^2 + v^2) - \Omega$ ,  $f_v = v - u(u^2 + v^2) - \Omega - F_d$ , and  $F_d = f_d(3|\gamma|)^{1/2}/[2(\omega\Delta\omega)^{3/2}]$ . Eq. (5) can be solved numerically [32] to obtain the average escape time that coincides with the inverse of the

sought Poissonian rate. The numerical results for  $E_a$  and  $\Gamma_0$  are shown in Fig. 4 in open (blue) triangles.

One can see that the exact (numerical) result has the same power law dependence as the analytical results (dashed line), even where the approximate theory is not supposed to hold. Quantitative agreement between experiment and theory on  $E_a$  is obtained with  $C \approx 1.3$ , thus validating the experimental noise amplitude calibration to within 15 % which is remarkable. Note that the simulation does not contain any other free parameter, which are all experimentally known to better than 5 %. Concerning  $\Gamma_0$ , we are not aware of previous attempts to compare this quantity to the theoretical predictions. The agreement with the full theory is within a factor of about 3, which is remarkable given the logarithmic precision on this parameter. We speculate that these discrepancies could arise from the actual algorithm used to extract  $\Gamma_0$ , or from more fundamental reasons like extra (non-Duffing) nonlinearities appearing in Eq. (2) (i.e. non-linear damping, or non-cubic restoring force terms) [35].

In conclusion, we have investigated the escape dynamics close to the bifurcation point for a nanomechanical resonator in the Duffing non-linear regime measured at cryogenic temperatures. Using a *single ideally tunable system*, we have: (i) Measured the escape rate  $\Gamma$  as a function of the noise amplitude  $D$ , the detuning to the bifurcation point  $\omega - \omega_b$ , and the nonlinear parameter  $\gamma$ . (ii) Extracted  $E_a$  and  $\Gamma_0$  as defined by Eq. (1). (iii) Verified that the universal scaling of  $E_a$  and  $\Gamma_0$  initially predicted for a tiny region around the bifurcation point holds actually in a region up to two orders of magnitude larger than the original one. (iv) Verified by solving numerically the exact problem, that the observation is in quantitative agreement with the behavior expected for a driven Duffing oscillator. The scaling of  $E_a$  as a function of  $|\Omega - \Omega_b|$  is consistent with the predictions of Refs.



[18, 19]. Due to the generality of the Duffing model, these results are of interest for a wide class of systems. Even beyond the fundamental interest in the scaling laws we point out that the device acts as a very sensitive amplifier: it allows the detection of tiny variations of the resonator frequency. Understanding the frequency fluctuations in mechanical resonators is a current challenge of the field [27–29]. Mastering of the bifurcation escape technique by having a reliable theory and experimental

verification of the scaling of the rates is a crucial step towards the study of modifications induced by other phenomena.

We gratefully acknowledge discussions with M. Dykman, K. Hasselbach, E. Lhotel and A. Fefferman. We thank J. Minet and C. Guttin for help in setting up the experiment. We acknowledge support from MICROKELVIN, the EU FRP7 grant 228464 and of the French ANR grant QNM n° 0404 01.

- 
- [1] S. Arrhenius, Z. Physik. Chem. **4**, 226 (1889).
  - [2] H. A. Kramers, Physica **7**, 284 (1940).
  - [3] M. A. Novak, R. Sessoli, A. Caneschi, and D. Gatteschi, J. of Magn. and Magn. Mater. **146**, 211 (1995).
  - [4] E. M. Ozbudak, M. Thattai, H. N. Lim, B. I. Shraiman, and A. van Oudenaarden, Nature **427**, 737 (2004).
  - [5] E. A. Dethoff, J. Chugh, A. M. Mustoe, and H. M. Al-Hashimi, Nature **482**, 322 (2012).
  - [6] E. Turlot, D. Esteve, C. Urbina, J. M. Martinis, M. H. Devoret, S. Linkwitz, and H. Grabert, Phys. Rev. Lett. **62**, 1788 (1989).
  - [7] J. Kurkijarvi, Phys. Rev. B **6**, 832 (1972).
  - [8] L. J. Lapidus, D. Enzer, and G. Gabrielse, Phys. Rev. Lett. **83**, 899 (1999).
  - [9] I. Siddiqi, R. Vijay, F. Pierre, C. M. Wilson, M. Metcalfe, C. Rigetti, L. Frunzio, and M. H. Devoret, Phys. Rev. Lett. **93**, 207002 (2004).
  - [10] J. S. Aldridge and A. N. Cleland, Phys. Rev. Lett. **94**, 156403 (2005).
  - [11] C. Stambaugh and H. B. Chan, Phys. Rev. B **73**, 172302 (2006).
  - [12] H. B. Chan and C. Stambaugh, Phys. Rev. Lett. **99**, 060601 (2007).
  - [13] H. B. Chan, M. I. Dykman, and C. Stambaugh, Phys. Rev. Lett. **100**, 130602 (2008).
  - [14] Q. P. Unterreithmeier, T. Faust, and J. P. Kotthaus, Phys. Rev. B **81**, 241405 (2010).
  - [15] N. Boulant, G. Ithier, P. Meeson, F. Nguyen, D. Vion, D. Esteve, I. Siddiqi, R. Vijay, C. Rigetti, F. Pierre, and M. Devoret, Phys. Rev. B **76**, 014525 (2007).
  - [16] P. Hänggi, P. Talkner, and M. Borkovec, Rev. Mod. Phys. **62**, 251 (1990).
  - [17] M. I. Dykman and M. A. Krivoglaz, Sov. Phys. JETP, **60** (1979).
  - [18] M. Dykman, I. Schwartz, and M. Shapiro, Phys. Rev. E **72**, 021102 (2005).
  - [19] O. Kogan, arXiv:0805.0972v2 (2008).
  - [20] E. Collin, M. Defoort, K. Lulla, T. Moutonet, J.-S. Heron, O. Bourgeois, Y. M. Bunkov, and H. Godfrin, Review of Scientific Instruments **83**, 045005 (2012).
  - [21] A. Cleland and M. Roukes, Sensors and Actuators **72**, 256 (1999).
  - [22] E. Collin, T. Moutonet, J.-S. Heron, O. Bourgeois, Y. M. Bunkov, and H. Godfrin, J Low Temp Phys **162**, 653 (2011).
  - [23] I. Kozinsky, H. W. C. Postma, I. Bargatin, and M. L. Roukes, Applied Physics Letters **88**, 253101 (2006).
  - [24] S. Zaitsev, O. Shtempluck, E. Buks, and O. Gottlieb, Nonlinear Dynamics **67**, 859 (2012).
  - [25] E. Collin, T. Moutonet, J.-S. Heron, O. Bourgeois, Y. M. Bunkov, and H. Godfrin, Phys. Rev. B **84**, 054108 (2011).
  - [26] E. Collin, Y. M. Bunkov, and H. Godfrin, Phys. Rev. B **82**, 235416 (2010).
  - [27] K. Y. Fong, W. H. P. Pernice, and H. X. Tang, Phys. Rev. B **85**, 161410(R) (2012).
  - [28] Y. Zhang, J. Moser, J. Güttinger, A. Bachtold, and M. I. Dykman, Phys. Rev. Lett. **113**, 255502 (2014).
  - [29] R. van Leeuwen, A. Castellanos-Gomez, G. Steele, H. van der Zant, and W. Venstra, Appl. Phys. Lett. **105**, 041911 (2014).
  - [30] W. Eadie, D. Drijard, F. James, M. Roos, and B. Sadoulet, *Statistical Methods in Experimental Physics*, edited by North-Holland (Amsterdam, 1971).
  - [31] M. Defoort, *PhD thesis: Non-linear dynamics in nano-electromechanical systems at low temperature* (CNRS et Université Grenoble Alpes, unpublished, 2014).
  - [32] F. Pistolesi, Y. Blanter, and I. Martin, Physical Review B **78**, 085127 (2008).
  - [33] We can estimate adiabaticity using theoretical expressions from Ref. [24]. Eqs. (50), (53) and (57) give the shift in bifurcation frequency  $\delta_{err}$  induced by finite sweep rate. We obtain  $\delta_{err} = 2\pi 0.5$  Hz at most with our experimental parameters, which means that the error in the resonance position is less than 20 ppm of the Duffing frequency shift itself. At the same time, the critical slowing down time  $\tau_{sd}$  can be estimated from Eq. (52). We obtain  $\tau_{sd}$  smaller than 8 ms for all our settings, which shall be compared to the smallest recorded bifurcation time of order 40 ms.
  - [34] These expressions are obtained following the method of Ref. [17]. Note that in our work the bifurcation is analysed as a function of frequency detuning and nonlinear parameter (not applied force).
  - [35] We tried to quantify the impact of nonlinear damping and of gate coupling non-Duffing contributions on the dynamics equation. Using a quadratic fit to describe nonlinear damping [25, 26], one can estimate the  $p$  parameter of Ref. [24] to be at worst about 0.06. Following the calculation procedure of Ref. [17], the alteration of the energy potential  $E_a$  is then at worst about 20 %. From the gate capacitance Taylor series coefficients of Ref. [20], we calculate that the "effective" Duffing nonlinear parameter measured in a frequency-sweep experiment could be modified by about 4 % with respect to the value computed from the actual  $x^3$  restoring force term, which is small.